Natural antisense transcript of *Period2*, *Per2AS*, regulates the amplitude of the mouse circadian clock

Rebecca A. Mosig,[1,2] Allison N. Castaneda,[1,2] Jacob C. Deslauriers,[1,2] Landon P. Frazier,[1,2] Kevin L. He,[1,2] Naseem Maghzian,[1,2] Aarati Pokharel,[1,2] Camille T. Schrier,[1,2,3] Lily Zhu,[1,2] Nobuya Koike,[4] John J. Tyson,[1,2,3] Carla B. Green,[5] Joseph S. Takahashi,[5,6] and Shihoko Kojima[1,2,3]

[1]Department of Biological Sciences, Virginia Polytechnic Institute and State University, Blacksburg, Virginia 24061, USA; [2]Fralin Life Sciences Institute, Virginia Polytechnic Institute and State University, Blacksburg, Virginia 24061, USA; [3]Division of Systems Biology, Academy of Integrated Science, Virginia Polytechnic Institute and State University, Blacksburg, Virginia 24061; [4]Department of Physiology and Systems Bioscience, Kyoto Prefectural University of Medicine, Kyoto 062-8566, Japan; [5]Department of Neuroscience, The University of Texas Southwestern Medical Center, Dallas Texas 75390, USA; [6]Howard Hughes Medical Institute, The University of Texas Southwestern Medical Center, Dallas, Texas 75390, USA

In mammals, a set of core clock genes form transcription–translation feedback loops to generate circadian oscillations. We and others recently identified a novel transcript at the *Period2* (*Per2*) locus that is transcribed from the antisense strand of *Per2*. This transcript, *Per2AS*, is expressed rhythmically and antiphasic to *Per2* mRNA, leading to our hypothesis that *Per2AS* and *Per2* mutually inhibit each other's expression and form a double negative feedback loop. By perturbing the expression of *Per2AS*, we found that *Per2AS* transcription, but not transcript, represses *Per2*. However, *Per2* does not repress *Per2AS*, as *Per2* knockdown led to a decrease in the *Per2AS* level, indicating that *Per2AS* forms a single negative feedback loop with *Per2* and maintains the level of *Per2* within the oscillatory range. *Per2AS* also regulates the amplitude of the circadian clock, and this function cannot be solely explained through its interaction with *Per2*, as *Per2* knockdown does not recapitulate the phenotypes of *Per2AS* perturbation. Overall, our data indicate that *Per2AS* is an important regulatory molecule in the mammalian circadian clock machinery. Our work also supports the idea that antisense transcripts of core clock genes constitute a common feature of circadian clocks, as they are found in other organisms.

[*Keywords*: Period2; amplitude; antisense transcript; circadian; long noncoding RNA]

Supplemental material is available for this article.

Received August 20, 2020; revised version accepted April 26, 2021.

Eukaryotic genomes are pervasively transcribed, and non-protein-coding portions of the genome dominate the transcriptional output of mammals (Bertone et al. 2004; Røsok and Sioud 2004; Carninci et al. 2005; Katayama et al. 2005; Sun et al. 2006). RNA species beyond mRNA are known as noncoding RNAs (ncRNAs) and have been categorized into many subtypes, such as ribosomal RNA (rRNA), transfer RNA (tRNA), small nucleolar RNAs (snoRNAs), small nuclear RNAs (snRNAs), microRNAs (miRNAs), circular RNAs (circRNAs), and long noncoding RNAs (lncRNAs) (for review, see Mercer et al. 2009; Panda et al. 2017). Despite their pervasive transcription, ncRNAs, particularly lncRNAs, were originally considered to be mere transcriptional noise and to lack defined functions. Poor evolutionary conservation in their primary sequences between species also raised concerns about their functional significance (Ponjavic et al. 2007; Guttman et al. 2009; Johnsson et al. 2014). More recent studies, however, have revealed an intriguing conservation of the genomic positions of lncRNAs (i.e., synteny) as well as conservation of their promoter and exon sequences, compared with intron or nontranscribed intergenic regions of protein-coding genes (Khaitovich et al. 2006; Pang et al. 2006; Yassour et al. 2010; Rhind et al. 2011; Derrien et al. 2012; Goodman et al. 2013; Anderson et al. 2016; Engreitz et al. 2016; Groff et al. 2016). These observations raise the possibility that some lncRNAs, if not all, are biologically relevant and have important and conserved functions. Indeed, a few dozen examples have highlighted the importance of lncRNAs in a variety of

Corresponding author: skojima@vt.edu
Article published online ahead of print. Article and publication date are online at http://www.genesdev.org/cgi/doi/10.1101/gad.343541.120.

biological processes, such as X chromosome inactivation, imprinting, cell cycle regulation, and stem cell differentiation (Lee et al. 1999; Smilinich et al. 1999; Sleutels et al. 2002; Feng et al. 2006; Dinger et al. 2008; Morris et al. 2008; Zhao et al. 2008; Bond et al. 2009; Sopher et al. 2011; Modarresi et al. 2012).

Circadian rhythmicity, which modulates daily biochemical, physiological, and behavioral cycles, is a fundamental aspect of life on Earth. In mammals, essentially every cell is capable of generating circadian rhythms, and, within each cell, a set of clock genes forms a network of transcription-translation feedback loops that drive oscillations of ~24 h (for review, see Lowrey and Takahashi 2004; Takahashi et al. 2008; Takahashi 2017). In one of these loops, the heterodimeric transcription activators (BMAL1/CLOCK and its paralog BMAL1/NPAS2) activate transcription of the *Period* (*Per*) *1-3* and *Cryptochrome (Cry) 1-2* genes, resulting in high levels of these transcripts. The resulting PER and CRY proteins then heterodimerize in the cytoplasm, translocate back to the nucleus, and interact with CLOCK/BMAL1 to inhibit transcription of *Per* and *Cry* genes. Subsequently, the PER/CRY repressor complex is degraded, and BMAL1/CLOCK can now activate a new cycle of transcription. In a second feedback loop, BMAL1/CLOCK activates the expression of orphan nuclear receptor genes *Rev-erbα/β* (*Nr1d1/2*). REV-ERB proteins in turn repress the expression of *Bmal1*, *Clock, Npas2, Cry1*, and *Nfil3*. ROR proteins, also orphan nuclear receptors, recognize the same DNA motif as REV-ERB proteins, compete with their binding, and activate the expression of the same target genes. In the last loop, BMAL1/CLOCK activates the expression of *Dbp*, while REV/ROR proteins activate and inhibit the expression of *Nfil3,* respectively. Both DBP and NFIL3 are transcription factors: DBP activates while NFIL3 represses the transcription of target genes, such as *Rev-erbs, Rors*, and *Pers.* These feedback loops constitute the molecular mechanism, as currently understood, of circadian rhythms in mammals (for review, see Takahashi 2017).

Several circadian transcriptome studies discovered a new RNA molecule, which we named *Per2AS,* that is transcribed within the *Per2* locus in mouse liver, lung, kidney, and adrenal gland (Koike et al. 2012; Menet et al. 2012; Vollmers et al. 2012; Fang et al. 2014; Zhang et al. 2014). In mammals, 25%–40% of protein-coding genes have antisense transcript partners (Røsok and Sioud 2004; Katayama et al. 2005; Sun et al. 2006), and some antisense transcripts have been shown to exert functions in a variety of processes, such as cell cycle regulation, genome imprinting, immune response, neuronal function, and cardiac function (Faghihi and Wahlestedt 2009; Khorkova et al. 2014; Wanowska et al. 2018). However, the physiological roles of most antisense transcripts remain uncertain.

In an earlier study, we mathematically tested the hypothesis that *Per2AS* and *Per2* mutually inhibit each other's expression and form a double negative feedback loop, considering three potential mechanisms to describe the *Per2AS-Per2* interaction: transcriptional (i.e., transcriptional interference in *cis*), post-transcriptional (i.e., degradation of RNA duplexes in *trans*), or a combination of both effects. The model predicted that all three mechanisms are consistent with the basic molecular details of circadian rhythms in mouse but that the transcriptional model would lead to a more robust oscillation compared with the post-transcriptional model (Battogtokh et al. 2018).

In this study, we experimentally tested the predictions of these models by perturbing *Per2AS* expression both transcriptionally and post-transcriptionally. We found that *Per2AS* transcriptionally represses *Per2,* indicating that one of the functions of *Per2AS* is to maintain the level of *Per2* within an oscillatory range. This is critical, as *Per2* is the only core clock gene for which the abundance, rhythmicity, and the phase of its expression are critical to maintain circadian rhythmicity in mouse (Chen et al. 2009). We also found that *Per2AS* regulates the amplitude of the circadian clock, and this function does not rely solely on its interaction with *Per2*. Little is known about the molecular basis of circadian amplitude regulation, although the second feedback loop consisting of *Bmal1, Clock, Rev-erbα/β, Ror* genes has been implicated to play a central role (Vitaterna et al. 2006; He et al. 2016; Zhao et al. 2016; Littleton et al. 2020). As we establish *Per2AS* as a new player in amplitude regulation, functional analysis of *Per2AS* will help us deepen our understanding of the regulatory mechanisms of circadian amplitude. Overall, we propose that *Per2AS* serves as an important regulatory molecule in the mammalian circadian clock machinery.

Results

Characterization of Per2AS

Recent circadian transcriptome studies have identified a novel transcript, *Per2AS*, at the *Per2* locus that is transcribed from the opposite strand and expressed antiphasic to the sense *Per2* transcript in mouse liver (Koike et al. 2012; Menet et al. 2012; Vollmers et al. 2012; Fang et al. 2014; Zhang et al. 2014). Our quantitative PCR (qPCR) analyses demonstrated that the *Per2AS* is indeed expressed rhythmically and antiphasic to *Per2* mRNA in mouse liver, and it peaks at ZT 4 (Zeitgeber time, where ZT 0 and ZT 12 are defined as time of lights on and lights off, respectively) (Fig. 1A). Rhythmic and antiphasic expression patterns of *Per2AS* and *Per2* have been observed as well in NIH3T3 cells (*Bmal1*-luc) and mouse embryonic fibroblasts (MEFs) derived from *PER2::LUCIFERASE* knock-in mouse (Fig. 1A; Yoo et al. 2004).

Per2AS is spliced and polyadenylated, similar to mRNAs (Fig. 1B; Supplemental Fig. S1A). Rapid Amplification of cDNA Ends (RACE) analysis revealed that the transcription start site (TSS) of *Per2AS* is located in intron 6 of *Per2* (Fig. 1B), which is consistent with the most 5′ signals of *Per2AS* (Supplemental Fig. S1A; Koike et al. 2012; Menet et al. 2012; Zhang et al. 2014). Strong and rhythmic recruitment of RNAPII-Ser5P (RNA polymerase II whose serine 5 in the C-terminal domain is phosphorylated) has been observed just upstream of *Per2AS* TSS, indicating an active and rhythmic initiation of transcription at this site

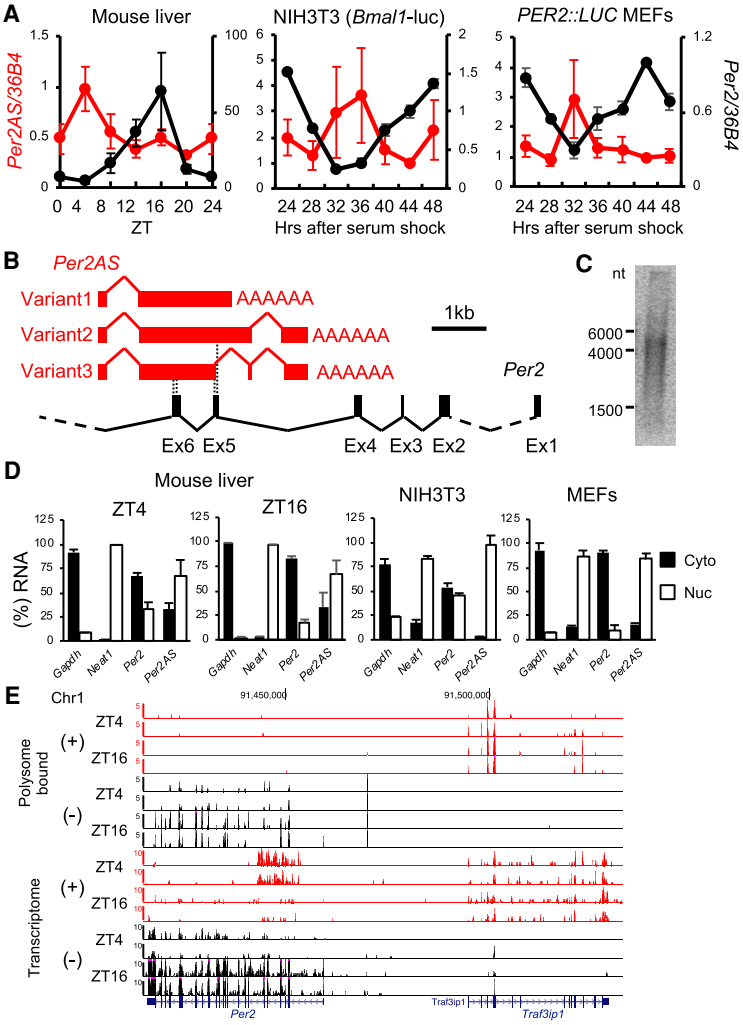

Figure 1. Characterization of *Per2AS*. (*A*) Relative RNA expression of *Per2AS* (red) and *Per2* (black) in mouse liver, *Bmal1-luc* (NIH3T3), and *PER2::LUC* MEFs. The expression levels of *Per2AS* at 44 h after serum shock were set to 1 in *Bmal1-luc* and *PER2::LUC* MEFs. (*B*) Genomic structure of *Per2AS* (red) in relation to *Per2* (black). Dotted lines indicate the regions where the exons of *Per2* and *Per2AS* overlap. (*C*) Northern blot analysis of *Per2AS*. PolyA$^+$ enriched RNA was extracted from mouse liver at ZT 4 and probed with *Per2AS* sequence (1–1812 nt that are shared in all the variants, depicted in *B*). Numbers on the left represent the size of RNA markers. (*D*) Subcellular localization of *Per2AS* and *Per2* RNAs in mouse liver at ZT 4 or at ZT 16, NIH3T3 cells and MEFs. (*Neat1*) Nuclear RNA, (*Gapdh*) cytoplasmic RNA serving as controls. (*E*) Genome browser view on Chromosome 1 for both ribosome-bound transcripts (*top*) and ribosome-depleted RNAs (*bottom*). Data analyzed are from Janich et al. (2015). All the data represent mean ± SEM (n = 2-5).

(Supplemental Fig. S1A; Phatnani and Greenleaf 2006). RNAPII's recruitment pattern also coincides with the expression pattern of *Per2AS* (Supplemental Fig. S1B), indicating that *Per2AS* is transcribed by RNAPII.

Per2AS consists of at least three variants ranging in size from ~2000 to 3500 nt (Fig. 1B), while Northern blot analysis yielded a strong signal around ~5000 nt (Fig. 1C). Given that the signal from Northern blot was smeared, ranging from ~1500 to 5000 nt (Fig. 1C), and the *Per2AS* signals from circadian transcriptome studies were detected in a ≥10-kb range (Supplemental Fig. S1A; Koike et al. 2012; Menet et al. 2012; Zhang et al. 2014), *Per2AS* presumably has many variants that are different in splicing patterns and transcription termination sites.

All three *Per2AS* variants that we detected by RACE have a potential to encode a small protein (the longest ORF common to all three is 291 nt; 97 amino acids); however, the potential polypeptide has no sequence similarity to any existing or predicted polypeptides in the GenBank protein database or the Conserved Domain Database. Furthermore, the Coding Potential Calculator (http://cpc.cbi.pku.edu.cn) predicts that *Per2AS* does not encode a protein, as the coding score of *Per2AS* is much smaller (from −0.97 to −0.99 depending on variant) than that of *Per2* (17.53). Furthermore, *Per2AS* transcripts are predominantly detected in the nucleus in mouse liver both at ZT4 and ZT16 (the peak and trough times of *Per2AS*, respectively), NIH3T3 cells, and MEFs (Fig. 1D), similar to *Neat1*, a lncRNA known to localize in the nucleus (Clemson et al. 2009). In contrast, protein-coding transcripts, such as *Gapdh* and *Per2*, were localized largely in the cytoplasm in order for them to be translated (Fig. 1D). In addition, *Per2AS* is not bound to polysomes and therefore not actively translated, in contrast to *Per2* that shows strong signals both in ribosome profiling and transcriptome data, and those signals are higher at ZT16 compared with ZT4 (Fig. 1E; Supplemental Fig. S1C; Atger et al. 2015; Janich et al. 2015). The neighboring protein-coding transcript, *Traf3ip1*, that is transcribed from the same strand as *Per2AS*, also showed a clear signal both in ribosome profiling and transcriptome data, eliminating the possibility that lack of *Per2AS* signals in the polysome-bound fraction is due

to its strand. These data collectively indicate that *Per2AS* is a long noncoding antisense transcript and does not produce a protein.

Per2AS regulates Per2 and the amplitude of the circadian clock

To understand the functional relevance of *Per2AS* in the mammalian circadian clock, we first used CRISPR technology to perturb *Per2AS* expression. We targeted the putative *Per2AS* promoter region, defined by the strong and rhythmic recruitment of RNAPII-Ser5P spanning ~900 bp (Supplemental Fig. S1A,B). We introduced CRISPR mutagenesis in two independent cell lines: MEFs from *PER2::LUCIFERASE* (*PER2::LUC*) knock-in reporter mice, in which a luciferase gene is fused to the 3′ end of the endogenous *Per2* gene (Yoo et al. 2004), and *Bmal1*-luc, an NIH3T3-derived luciferase-reporter cell line that has been stably transfected by a luciferase gene driven by the *Bmal1* promoter (Morf et al. 2012). Following single-cell sorting, we successfully isolated two *PER2::LUC MEF* (5D8 and 6F8) and one *Bmal1-luc* (mut8) mutant clones that had similar but distinct mutations at ~260 bp upstream of *Per2AS* TSS (Supplemental Fig. S1D). Because these cell lines were near tetraploid on average (Supplemental Fig. S1E), we not only identified the types of mutations but also calculated the frequency of each mutant allele in each mutant (Supplemental Fig. S1D). All the alleles were mutated in *PER2::LUC* 5D8 and 6F8, in which various deletions were detected (i.e., 11 bp, 3 bp, 2 bp, and 1 bp). Meanwhile in *Bmal1*-luc (mut8), only 29% of alleles had a mutation (6-bp deletion) and the remaining 71% were intact (Supplemental Fig. S1D). We also targeted five other regions within the *Per2AS* promoter, including TSS and the TATA-box-like sequence (TATAATCAA) located 63 bp upstream of the TSS; however, we were unable to isolate mutant clones, probably because these targeted regions were essential for cell survival or could not be easily accessed by the CRISPR machinery.

In these mutant cell lines, the level of *Per2AS* was up-regulated to 138% (5D8) and 325% (6F8) compared with the control (parental) cell line, as opposed to our expectations that *Per2AS* would be down-regulated. Nonetheless, the level of *Per2* was reduced to 57% (5D8) and 70% (6F8), respectively (Fig. 2A). Similarly, in *Bmal1-luc* mut8, the *Per2AS* level was up-regulated to 145%, while the *Per2* level was reduced to 76% (Fig. 2D). These data indicate that the DNA region ~260 bp upstream of the *Per2AS* TSS is important for *Per2AS* expression and that *Per2AS* represses *Per2*. Some long noncoding antisense transcripts modulate the expression of not only their target sense gene but also neighboring genes (Halley et al. 2014; Villegas et al. 2014). However, this was not the case for *Per2AS*, as the levels of *Ilkap*, *Hes6*, and *Traf3ip1*, the three closest genes, remained unchanged in all of our mutants (Supplemental Fig. S1F,G).

When we monitored the bioluminescent output from these mutant cells, the luminescent levels of both 5D8 and 6F8 were lower and their rhythmicity was less robust compared with the control (Fig. 2B; Supplemental Fig. S2A,B). Quantification analyses further revealed that the amplitude of 5D8 and 6F8 was decreased to 25%–30% and the period was ~1.5 h shorter compared with the control (Fig. 2C). In contrast, the bioluminescence signal from *Bmal1-luc* mut8 was markedly higher (Fig. 2E; Supplemental Fig. S2C,D); the amplitude was increased to 184% and the period was 0.9 h shorter compared with the control (Fig. 2F).

We also measured the level of BMAL1 and PER2 proteins in these *Per2AS* mutants and found that the level of BMAL1 protein was slightly elevated in all three mutants (Fig. 2G,H), consistent with the results from *Bmal1-luc* reporter output (Fig. 2E). We were unable to detect PER2::LUC protein (data not shown); however, PER2::LUC is a fusion protein in which a *luciferase* gene is fused in-frame to the 3′ end of the endogenous mouse *Per2* gene, and bioluminescent output is considered to represent the amount of PER2::LUC protein (Yoo et al. 2004; Chen et al. 2009; Yoo et al. 2017). In contrast, PER2 protein level was moderately increased in *Bmal1-luc* mut8 cells (Fig. 2G,H), despite the fact that the *Per2* mRNA level was decreased in this cell line. There are two plausible reasons to explain the increase in PER2: an off-target effect of CRISPR, or the compensation mechanism as the level of PER2 is critical to maintain circadian rhythmicity (Chen et al. 2009). We think the former unlikely, as none of the potential hits for off-targets in exon included clock genes, and translational regulation of PER2 has not been reported thus far, although we cannot fully exclude this possibility. We also think that changes in period are most likely due to the effect of *Per2AS* on *Per2*, as the period of a luciferase reporter output is shorter in mouse fibroblasts (Ramanathan et al. 2014), although the effect of *Per2* on circadian period in *Per2* KD/KO is highly variable between species, tissues, its expression level, and type of measurements (see the Discussion for more details).

To further characterize the *Per2AS* mutants as well as to gain insights into the underlying mechanisms of circadian amplitude regulation, we next measured the mRNA expression patterns of 13 core clock genes after synchronizing these cells by serum shock (Balsalobre et al. 1998). We found that the mRNA expression of *Bmal1*, *Cry1*, and *Rora* were elevated, while the expression of *Per2* was decreased in all three mutants (Fig. 3). The up-regulation of *Bmal1* mRNA level was consistent with the increased bioluminescence levels in *Bmal1-luc* cells and BMAL1 protein level (Fig. 2E,G,H). The mRNA expression of *Nfil3* was up-regulated in *PER2::LUC* 5D8 and *Bmal1-luc* mut8, while *Cry2* levels are higher in 5D8 and 6F8 than those in WT (Fig. 3, bottom left). Interestingly, the expression of *Npas2* was down-regulated in the *PER2::LUC* mutants but up-regulated in the *Bmal1-luc* mutant. No significant changes were observed for *Rev-erbα* and *Rev-erbβ* (Fig. 3). These data suggest that *Bmal1*, *Cry1*, *Rora*, *Per2* (changed in all three mutants), but not *Rev-erbα/β*, are involved in the *Per2AS*-mediated amplitude regulation.

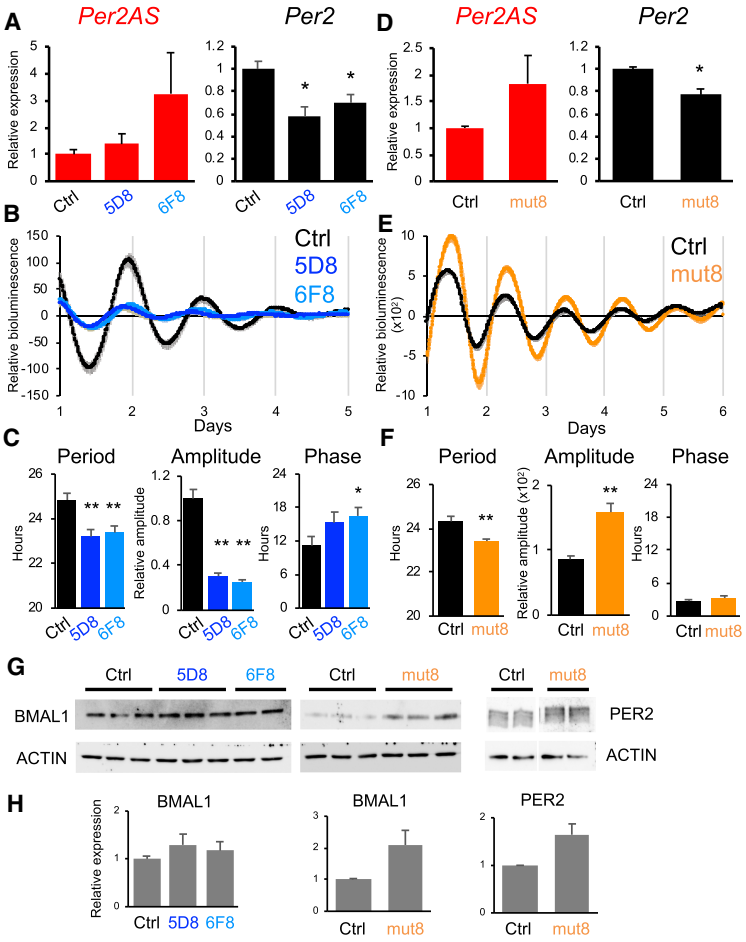

Figure 2. *Per2AS* mutants alter *Per2* and the amplitude of the circadian clock. (*A*,*D*) Relative expression levels of *Per2AS* (red), and *Per2* (black) in the *Per2AS* mutant cell lines of *PER2::LUC* MEFs ($n = 4$–6) (*A*) or *Bmal1-luc* (*D*) ($n = 13$). (*B*,*E*) Detrended bioluminescent output of the mutant cell lines of *PER2::LUC* MEFs (WT: $n = 13$, 5D8: $n = 13$, 6F8: $n = 13$) (*B*) or *Bmal1-luc* (WT: $n = 23$, mut8: $n = 23$) (*E*). Bold lines represent the mean, while shaded areas represent the SEM. (*C*,*F*) Period (*left*), amplitude (*middle*), and phase (*right*) of bioluminescent output calculated from *B* (*PER2::LUC* MEFs) or *E* (*Bmal1-luc*). (*G*) Representative images of Western blot analyses. (*H*) Quantification of BMAL1 and PER2 levels from Western blot analyses. All the data represent mean ± SEM. (*) $P < 0.05$, (**) $P < 0.005$ (Student's *t*-test).

Transcripts of Per2AS do not play a major role in the circadian clock machinery

In contrast to coding genes whose functional unit is an encoded protein, the functional unit of lncRNAs is often unknown. It can be the transcript itself (i.e., RNA molecule and/or the small ORF embedded in the sequence that has the potential to encode a protein) that regulates target mRNAs post-transcriptionally by affecting splicing, mRNA stability, mRNA localization, or epigenetic marks (Wight and Werner 2013; Khorkova et al. 2014). It can also be the very act of transcription, in which transcription of one strand suppresses transcription of another in *cis*, a process called transcription interference (Wight and Werner 2013; Khorkova et al. 2014).

To distinguish whether the functional unit of *Per2AS* is either a transcript (i.e., post-transcriptional model) or the act of transcription (i.e., pretranscriptional model) (Battogtokh et al. 2018), we post-transcriptionally decreased the level of *Per2AS* using "gapmers," chimeric antisense nucleotides containing modified nucleic acid residues to induce RNase H-mediated degradation of nuclear-retained RNA (Lee et al. 2012), as the majority of *Per2AS* RNA remains in the nucleus in fibroblasts (Fig. 1D) and RISC-mediated RNA cleavage triggered by siRNAs occurs mainly in the cytoplasm (Carthew and Sontheimer 2009). We also targeted gapmers to exon 1 of *Per2AS* (i.e., intron 6 of *Per2)* that was shared by all three variants (Fig. 1B). Gapmers 5 and 8 successfully reduced the level of *Per2AS* to 61% in *Bmal1-luc* cells (Fig. 4A); however, the level of *Per2* remained unchanged (Fig. 4A). Even though gapmers can not only induce RNA duplex-mediated degradation but also premature transcriptional termination of target mRNAs leading to reduced transcriptional activity and thereby confounding the interpretation of the results (Lee and Mendell 2020), this is unlikely the case for *Per2AS* gapmers, as the level of *Per2* is unaffected. Unexpectedly, however, gapmer-mediated *Per2AS* knockdown led to an ~20% reduction in the *Bmal1* level in *Bmal1-luc* cells (Fig. 4A).

We also post-transcriptionally overexpressed *Per2AS* using variant 2 (i.e., the longest variant) (Fig. 1B) in *Bmal1-luc* cells. This led to a marked increase in the *Per2AS* level by ~75,000-fold. Nevertheless, the *Per2* level remained unchanged, whereas the *Bmal1* level showed an approximate twofold increase (Fig. 4B). Knockdown or overexpression of *Per2AS* did not alter period, phase, or amplitude of bioluminescence output in *Bmal1-luc* cells (Fig. 4C). The change in *Bmal1* level was not due to comparable changes in the levels of *Rev-erbα/β* or *Rorα*, transcription repressor and activators of *Bmal1*, respectively (Fig. 4A,B; Sato et al. 2004). Rather, *Per2AS* appears

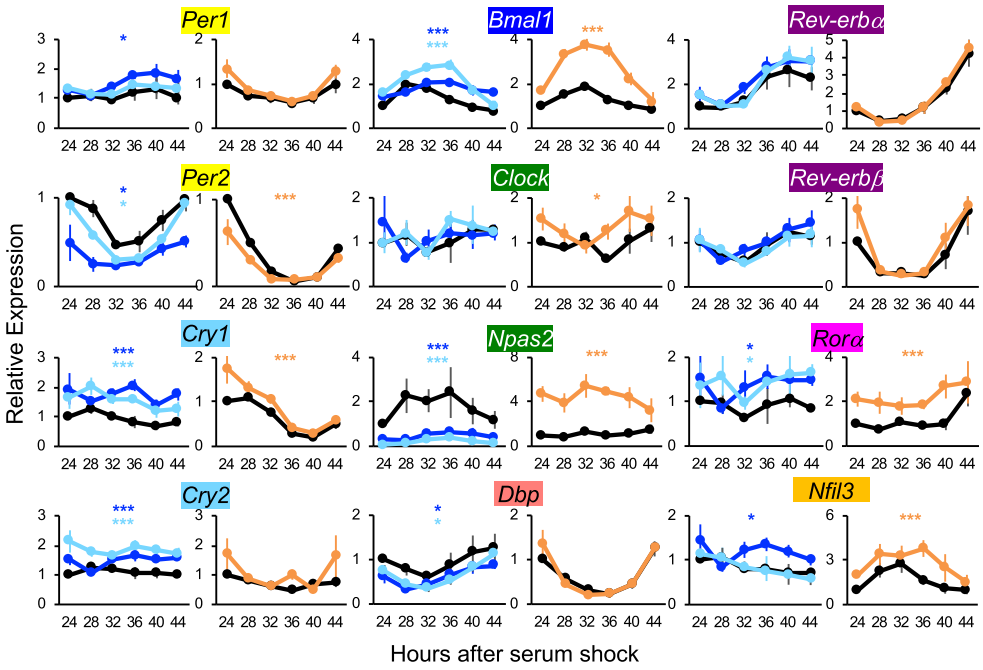

Figure 3. Relative expression levels of core clock genes in the *Per2AS* mutant cell lines. All the data represent mean SEM. *PER2::LUC* MEFs (WT: $n = 3$, 5D8: $n = 3$, 6F8: $n = 3$, color key in Fig. 2B) or *Bmal1-luc* (WT: $n = 3$, mut8: $n = 3$, color key in Fig. 2E). (*) $P < 0.05$, (***) $P < 0.005$ (two-way ANOVA).

to directly regulate the *Bmal1* transcription, as the increasing amount of *Per2AS* RNAs led to up-regulation of reporter activity of *Bmal1-luc* but not *Per2-luc* (Fig. 4D). Interestingly, however, the changes of *Bmal1* by *Per2AS* RNA was also cell type-specific, as it was not observed in *PER2::LUC* MEFs, even though the efficiency of *Per2AS* knockdown was higher (gapmer 5: 63%, gapmer 8: 60%) in *PER2::LUC* MEFs, compared with *Bmal1-luc* cells (both gapmers 5 and 8: 39%) (Supplemental Fig. S3). Overall, these data indicate that the transcript of *Per2AS* has little effect on the circadian control system (i.e., that its effects are not post-transcriptional). However, we also observed a small effect of *Per2AS* on *Bmal1* at least in *Bmal1-luc* cells, suggesting that *Per2AS* post-transcriptionally regulates *Bmal1* in a cell-specific manner.

Per2 knockdown down-regulates Per2AS and does not replicate the phenotypes of Per2AS CRISPR mutants

If *Per2AS* and *Per2* indeed form a double negative feedback loop and mutually inhibit each other's expression, then *Per2* mRNA knockdown would result in up-regulation of *Per2AS* level in the post-transcriptional model but no changes in the pretranscriptional model. To test this, we first reduced the level of *Per2* post-transcriptionally using shRNAs. Our *Per2* knockdown successfully reduced the level of *Per2* to 65% in AML12 cells, a mouse hepatocyte cell line, and 45% in *Bmal1-luc* cells (Fig. 5A,F). *Per2* knockdown also led to a decrease in the amplitude of bioluminescence output in *PER2::LUC* MEFs but not in *Bmal1-luc* cells (Fig. 5B–D). Period remained unchanged upon *Per2* knockdown in both cells, despite that previous studies in murine fibroblast and hepatocyte cell lines reported that circadian period became shorter upon *Per2* knockdown (Ramanathan et al. 2014). The residual *Per2* level is higher in our system compared with those reports (45% vs. 20%), and this could have contributed to the difference observed in our study. Nevertheless, *Per2* knockdown resulted in a decrease of the *Per2AS* level to 55% (Fig. 5A), contrary to either of our expectations (i.e., pretranscriptional or post-transcriptional interference).

We also measured the expression patterns of the core clock genes upon *Per2* knockdown in *Bmal1-luc* cells to evaluate whether the changes observed in the *Per2AS* mutant cells (Fig. 3) were mediated entirely through *Per2AS*'s effect on *Per2*. *Per2* knockdown did not result in changes of *Bmal1* mRNA levels (Fig. 5F), consistent with the bioluminescent output from *Bmal1-luc* cells (Fig. 5D) but inconsistent with our observations in *Bmal1-luc* mut8 cells, in which *Bmal1-luc* bioluminescence and *Bmal1* mRNA level were both significantly increased (Figs. 2E, 3). In addition, changes in mRNA expression patterns were observed only for *Nr1d2* and *Nfil3* upon *Per2* knockdown (Fig. 5F), in contrast to the changes in the mRNA expression patterns of *Cry1*, *Bmal1*, *Clock*, *Npas2*, *Rora*, and *Nfil3* observed in *Bmal1-luc* mut8 cells (Fig. 3). Interestingly, we did not observe any changes in mRNA levels of the core clock genes upon *Per2* knockdown in AML12 cells (Supplemental Fig. S4A), in which the level of *Per2AS* is ~100-fold higher compared with *Bmal1-luc* cells (Supplemental Fig. S4B). As the level of *Per2* was lower in *Bmal1-luc* with *Per2* knockdown (45%) compared

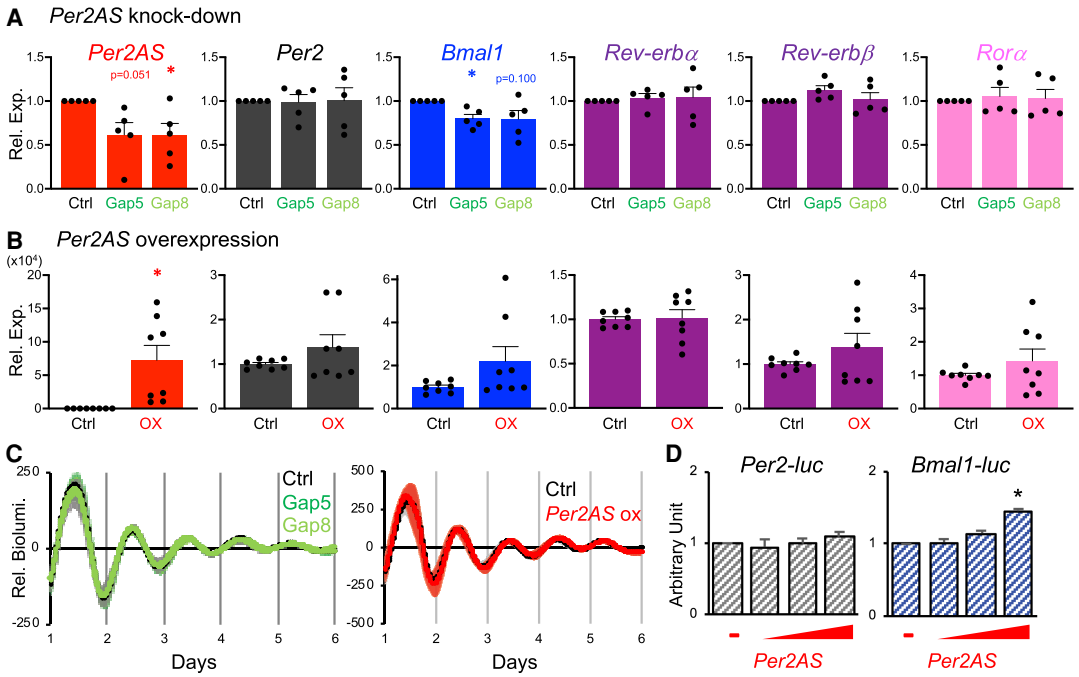

Figure 4. *Per2AS* transcripts regulate *Bmal1* but not *Per2* in *Bmal1-luc* cells. (*A*) Relative expression levels of core clock genes normalized by *36B4* upon *Per2AS* knockdown ($n = 5$). The values for controls were used as a reference and set at 1. (*B*) Relative expression levels of core clock genes normalized by *36B4* upon *Per2AS* overexpression ($n = 7$–8). All the data represent mean ± SEM. (*) $P < 0.05$. We excluded the samples that had <5000-fold induction of *Per2AS*. (*C*) Bioluminescent output from *Bmal1-luc* cells upon knockdown ($n = 8$) or overexpression ($n = 4$) of *Per2AS*. Bold lines represent the mean, while shaded areas represent the SEM. (*D*) Luciferase activity from *Per2-luc* or *Bmal1-luc* cotransfected with an increasing amount of *Per2AS* (variant2)-expressing plasmid.

with *Bmal1-luc* mut8 cells (75%), it is highly unlikely that changes in the mRNA expression patterns observed in *Bmal1-luc* mut8 cells (Fig. 3) are solely due to the *Per2-AS*'s effect on *Per2*. Rather, these data support the idea that *Per2AS* has a distinct role in the mammalian circadian system, independent of *Per2*.

Overall, our study has highlighted several important functions and regulatory mechanisms of *Per2AS* in the mammalian circadian clock system (Fig. 6): (1) *Per2AS* regulates circadian amplitude, (2) *Per2AS* employs both transcript- and transcription-dependent mechanisms, (3) the effect of *Per2AS* is both *Per2*-dependent and –independent, and (4) some of the functions and regulatory mechanisms of *Per2AS* are cell type-specific. Although the amplitude is an integral part of any cycling system, the molecular mechanisms of circadian amplitude regulation have remained enigmatic. Deepening our understanding how *Per2AS* functions in the circadian system will help us gain important insights into how the amplitude is regulated in the future.

Discussion

Based on the inverse expression patterns of *Per2AS* and *Per2*, we originally hypothesized that *Per2AS* and *Per2* mutually inhibit each other's expression and form a double negative feedback loop for *Per2AS* to exert its function. The experimental observations from this study bear out the assumptions underlying our mathematical models of *Per2-Per2AS* interactions, in which *Per2AS* and *Per2* mutually inhibit each other either transcriptionally or post-transcriptionally, or a combination of both effects (Battogtokh et al. 2018). Our experimental interrogation clearly demonstrated that *Per2AS* represses *Per2* (Fig. 2A,D), presumably via a transcriptional mechanism, as the knockdown or overexpression of *Per2AS* transcripts did not alter the level of *Per2* mRNAs (Figs. 4, 6). Contrary to our expectation, however, *Per2* positively regulates *Per2AS*, as the knockdown of *Per2* led to down-regulation (rather than up-regulation) of *Per2AS* (Fig. 5A). This effect is post-transcriptional, because the level of *Per2* pre-mRNA remained unchanged upon *Per2* knockdown (Supplemental Fig. S4C). We think it is unlikely that *Per2* RNA and *Per2AS* RNA form an RNA duplex and stabilize each other, because (1) the expression of *Per2AS* and *Per2* are antiphasic in at least some tissues (Fig. 1A; Zhang et al. 2014), (2) *Per2* is ~25 times more abundant than *Per2AS* (Fig. 1A; Koike et al. 2012), (3) *Per2* predominantly localizes in the cytoplasm while *Per2AS* localizes in the nucleus (Fig. 1D), and (4) *Per2AS* consists of many variants and their nucleotide sequences vary (Fig. 2E). Rather we favor the hypothesis that PER2 indirectly or directly regulates *Per2AS* transcription. In fact, REV-ERBα/β and BMAL1/CLOCK/PER1/PER2/CRY2 are recruited to the vicinity of the *Per2AS* TSS (Koike et al. 2012), potentially involved in regulating *Per2AS* transcription. Regardless of the mechanism, *Per2* is the only core clock gene whose

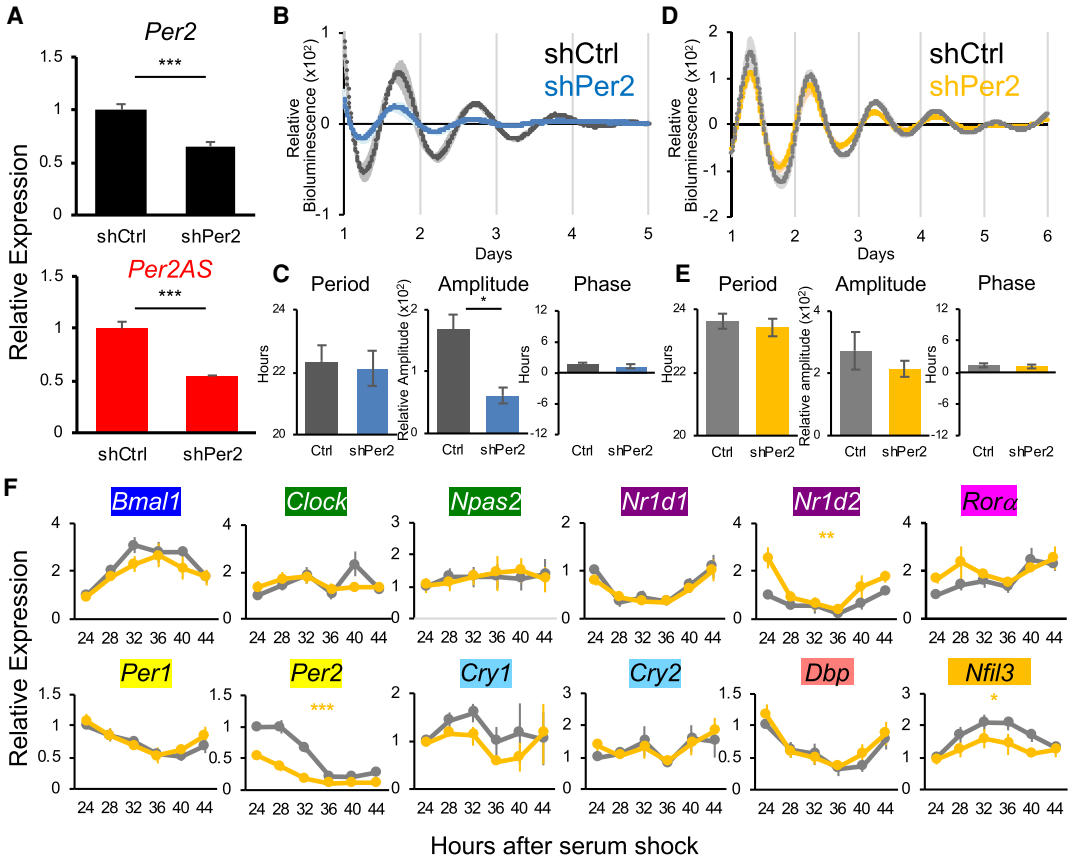

Figure 5. *Per2* knockdown does not replicate the phenotypes of *Per2AS* mutants. (*A*) Relative expression levels of *Per2* (*top*) and *Per2AS* (*bottom*) in the AML12 mouse hepatocytes ($n = 4$-5). (*B*,*D*) Relative bioluminescence output from *PER2::LUC* MEFs (*B*) ($n = 12$) or *Bmal1-luc* (*D*) ($n = 14$) upon *Per2* knockdown. (*C*,*E*) Period (*left*), amplitude (*middle*), and phase (*right*) of bioluminescent output calculated from *B* (*PER2::LUC* MEFs) or *D* (*Bmal1-luc*). (*F*) Relative expression levels of core clock genes in *Bmal1-luc* cells upon *Per2* knockdown ($n = 3$–5). All the data represent mean ± SEM. (*) $P < 0.05$, (***) $P < 0.005$ (two-way ANOVA).

rhythmicity, proper phase, and expression levels are all critical to sustain rhythmicity (Zheng et al. 1999; Bae et al. 2001; Chen et al. 2009). This study demonstrates that *Per2AS* serves as an additional regulatory mechanism to further ensure that *Per2*'s expression pattern stays within a certain window for sustaining robust circadian rhythmicity.

Our mathematical models were also constrained by the requirement that the expression of *Per2AS* and *Per2* are both rhythmic and antiphasic (180° out of phase). These patterns have been observed not only in liver but also in adrenal gland, lung, and kidney (Zhang et al. 2014). Analysis of mouse ENCODE data sets demonstrated that *Per2AS* is also expressed in many other tissues, such as genital and subcutaneous fat pad, bladder, kidney, colon, duodenum, large and small intestines, stomach, lung, and potentially in mammary gland, ovary, and testis (Supplemental Fig. S5A; The ENCODE Project Consortium 2012; Davis et al. 2018), although it is unclear whether *Per2AS* expression is rhythmic and antiphasic to *Per2* in these tissues. A *Per2AS* signal has not been detected in the central nervous system and a few other peripheral tissues including heart, placenta, spleen, and thymus (Supplemental Fig. S5A; The ENCODE Project Consortium 2012; Davis et al. 2018). These results could be due to tissue sampling times (i.e., little or no *Per2AS* may have been expressed when these tissues were harvested), or the *Per2AS* level was under the detection threshold, as the expression of lncRNAs is generally low (>10-fold lower than sense transcripts on average) and transcriptome analyses sometimes lack the sensitivity to detect all lncRNAs (He et al. 2008; Faghihi and Wahlestedt 2009; Xu et al. 2009; Xu et al. 2011; Djebali et al. 2012). Nevertheless, we recently reported that the level of *Per2AS* linearly correlates with that of *Rorc*, as well as the percentage of cycling genes among 12 mouse tissues (Littleton et al. 2020), indicating that *Per2AS* regulates the amplitude of the circadian transcriptome in these tissues, potentially with *Rorc*. These data also suggest that the functions of *Per2AS* is not limited to the cellular level (i.e., fibroblasts) but also extended to the physiological level. An antisense transcript of *Bmal1* was also detected in a few tissues, such as subcutaneous fat, bladder, kidney, colon, lung, and potentially in duodenum, stomach, mammary gland, and ovary (Supplemental Fig. S5B; The ENCODE Project Consortium 2012; Davis et al. 2018), as was also reported

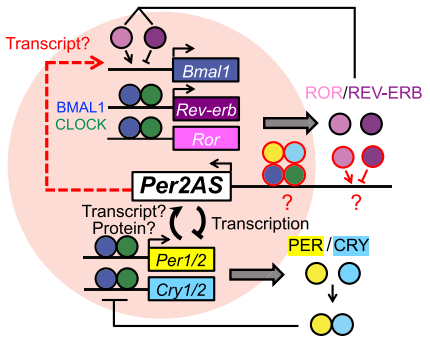

Figure 6. Putative model for the circadian molecular circuit including *Per2AS*. *Per2AS* and *Per2* form a single negative feedback where *Per2AS* limits the expression of *Per2* presumably pretranscriptionally. *Per2AS* can also activate the *Bmal1* expression post-transcriptionally (i.e., in *trans*) in a tissue- or cell-specific manner. Circadian transcription factors as well as PER-CRY protein complex may be recruited to the vicinity of the *Per2AS* TSS (Koike et al. 2012) to potentially regulate *Per2AS* transcription.

previously (Zhang et al. 2014). It would be of great interest to analyze whether the antisense transcript of *Bmal1* exerts some functions in the mammalian circadian clock system.

We also found that *Per2AS* regulates the amplitude of the circadian clock; however, *Per2AS* perturbation had an opposite effect on amplitude: a decrease in *PER2::LUC* reporter but an increase in *Bmal1-luc* reporter oscillations (Fig. 2). Because the amplitude is determined by the amplitude of either synthesis or degradation rates or a combination of both (Luck et al. 2014), the decrease of *PER2::LUC* reporter oscillations in the *Per2AS* mutants can be explained by the decreased amplitude of the *PER2::LUC* protein synthesis, triggered by the reduction of amplitude of *Per2* mRNA oscillation (Fig. 3). Interestingly, this is in spite of the increased level of BMAL1 protein (Fig. 2). In fact, the level of *Per2* pre-mRNA (an indicator of *Per2* mRNA synthesis) was reduced in all the mutant cell lines (Supplemental Fig. S7), evidence that *Per2* mRNA synthesis was decreased in *Per2AS* mutant cells. On the other hand, the increase of the amplitude of *Bmal1-luc* reporter oscillations is presumably due to the increase of *Bmal1* mRNA synthesis rate (Fig. 3).

The molecular basis of how *Per2AS* regulates amplitude still remains elusive. Recent studies have revealed that lncRNAs regulate target gene expression both via their transcripts and the act of transcription: Transcripts of lncRNA can regulate target gene expression by interacting with chromatin complexes, transcription factors, or their cofactors, whereas the act of transcription can also alter local chromatin structure as transcription machinery moves along DNA during transcription elongation or facilitate chromatin loop formation between transcription machinery at enhancers and promoters of distantly located target genes (Chen 2016; Marchese et al. 2017; Kaikkonen and Adelman 2018). Indeed, the act of transcription of *Per2AS* is necessary to regulate *Per2*, while both the transcript and the act of transcription are important to regulate *Bmal1*. Furthermore, the effect of the *Per2AS* transcript on *Bmal1* is cell type-specific (Fig. 4A,B; Supplemental Fig S3A), whereas that of transcription is presumably mediated by *Rora*, a *Bmal1* activator (Figs. 3, 6). Interestingly, there seem to be consistent effects on RORE-containing genes in the *Per2AS* mutants (Fig. 3), and this effect appears to be independent of *Per2*. *Per2* knockdown leads to decreased levels of RORE-controlled genes, such as *Bmal1*, *Cry1*, and *Nfil3* (Shearman et al. 2000; Schmutz et al. 2010; Ramanathan et al. 2014), whereas the levels of RORE-containing genes were up-regulated in the *Per2AS* mutants (Fig. 3), even though both conditions led to the decreased *Per2* level. In addition, the BMAL1 protein level was increased in the *Per2AS* mutants (Fig. 2) but remains unchanged with *Per2* KD (Supplemental Fig. S4D,E).

Our potential candidate for understanding the mechanisms of *Per2AS*-mediated amplitude regulation is *Rors*. Recent studies have also highlighted the role of the positive loop (*Clock-Arntl-Rev-Ror*) as the central axis of amplitude regulation (He et al. 2016; Zhao et al. 2016), and *Ror* genes have been shown to increase the circadian amplitude of molecular and behavioral rhythms (He et al. 2016). Furthermore, our recent study suggested that *Per2AS* and *Rorc* function synergistically in the circadian clock system and regulate the amplitude of circadian transcriptome output (Littleton et al. 2020). Understanding how transcript or transcription of *Per2AS* regulate RORE-containing genes may be the key to decipher how circadian amplitude is regulated.

We also observed phenotypic changes in period in addition to amplitude in the *Per2AS* mutants (Fig. 2), although it is unclear whether this is due to the changes in the level of *Per2* or a *Per2AS*-specific effect independent of *Per2*. The period phenotype observed by *Per2* KD/KO is highly variable between species, tissues, its expression level, and type of measurements (Ramanathan et al. 2014). For example, the period of a luciferase reporter output is shorter in NIH3T3 (mouse fibroblast) and MMH-D3 (mouse hepatocyte) cells, while it remains unchanged in 3T3-L1 (mouse adipocyte) cells when the *Per2* mRNA level was reduced to 20%–40% compared with the control (Ramanathan et al. 2014). However, the period is longer but with low amplitude in U2OS cells (human osteosarcoma cell line) when the *PER2* mRNA level is reduced to 20%–40% compared with the control (Baggs et al. 2009; Zhang et al. 2009). In $Per2^{-/-}$ mouse fibroblasts, the reporter output is arrhythmic and thus the period cannot be reliably quantified (Liu et al. 2007). In $Per2^{-/-}$ tissues, the period of *Per1-luc* bioluminescent output is shorter in the SCN, whereas it remained unchanged in pituitary or lung (Pendergast et al. 2010). The short period phenotype is not observed in the SCN of $Per2^{+/-}$ animals (-Pendergast et al. 2010). The free-running period of locomotor activity is either shorter or arrhythmic in $Per2^{-/-}$ mice (Zheng et al. 1999; Bae et al. 2001; Pendergast et al. 2010; Tamiya et al. 2016), while it is unchanged in $Per2^{+/-}$ mice (Pendergast et al. 2010; Tamiya et al. 2016). It is also worth noting that the *Per2AS* locus is disturbed in these $Per2^{-/-}$ and $Per2^{+/-}$ animals, confounding

the interpretation of the data (Zheng et al. 1999; Bae et al. 2001). These data collectively demonstrate that the relationship between *Per2* and the circadian period is not always as clear and straightforward as has been perceived and needs to be investigated further, with consideration of the interaction between *Per2AS* and *Per2*.

These experimental observations clearly indicate that our mathematical models need to be revised to better understand the functions and regulatory mechanisms of *Per2AS*. Specifically, the relationship between *Per2AS* and *Per2* is a single negative feedback loop, rather than a double negative feedback loop as we originally hypothesized. We also need to include the effect of *Per2AS* on *Bmal1*, as well as the potential effect of circadian transcription factors on *Per2AS* transcription (Fig. 6). Interestingly, a simpler mathematical model that involves only the core negative feedback loop where *Per2AS* and *Per2* mutually inhibit each other (Supplemental Fig. S6) supports the predictions from our original model, in which *Per2AS* would make the circadian oscillations more robust (Battogtokh et al. 2018). It will be of future interest to test whether the revised model also leads to the same conclusion.

Antisense transcripts of a core clock gene have also been reported in other organisms. In *Neurospora*, the sense *frequency* (*frq*) and antisense (*qrf*) transcripts are both located on the same chromosome and overlap almost completely (Kramer et al. 2003; Xue et al. 2014). In *Antheraea,* the sense–antisense transcripts for the homolog of *Drosophila*'s *period* (*per*) gene are located on different chromosomes (Sauman and Reppert 1996). Interestingly, human *PER2* also has an antisense transcript (*PER2AS*), but, based on human ENCODE data sets, the transcription of *PER2AS* and *PER2* diverges from their respective TSSs, most likely using a bidirectional promoter (Supplemental Fig. S5C; The ENCODE Project Consortium 2012; Davis et al. 2018). Although it is unclear whether all these sense-antisense transcripts have rhythmic and antiphasic expression patterns, the evolutionary conversation of sense–antisense pairs of a core clock gene suggests that antisense transcripts are part of a common mechanism for circadian clock regulation.

Even though the expression of *qrf* is rhythmic and antiphasic to *frq*, similar to *Per2AS* and *Per2* (Kramer et al. 2003; Xue et al. 2014), their functions in the core clock machinery appear to be different. *Frq* and *qrf* form a double negative feedback loop, and the primary function of *qrf* is to regulate phase and light entrainment in the presence of light and amplitude in the absence of light (Kramer et al. 2003; Xue et al. 2014). Because the molecular clock circuitry is markedly more complex in mammals than *Neurospora*, it is possible that *Per2AS* acquired additional or different functions, such as its apparent ability to regulate *Bmal1* in *trans*.

There is only limited experimental evidence about the functions and regulatory mechanisms of antisense transcripts, particularly in mammals. Most of the effort has been concentrated on understanding the function of antisense transcripts as an RNA molecule (transcript), and only a few studies have tested their function via transcriptional interference to regulate the sense gene expression. In addition, most of the studies have not analyzed the potential impact of the sense to the antisense transcript/transcription, despite the reciprocal regulation between sense and antisense transcripts being the most biologically intuitive mechanism. Our study contributes to an understanding of the possible functional roles of antisense transcripts by demonstrating that *Per2AS* is an important molecule to not only maintain the level of *Per2* within the oscillatory range but also to regulate the amplitude of the circadian clock. It would be of great interest to explore the functions of *Per2AS* at the tissue and organismal levels in the future.

Materials and methods

Tissue harvesting and cell culture

Male C57BL/6J mice were maintained on a 12:12 LD cycle and fed ad libitum, and livers were collected at the time indicated. All the animal experiments were conducted according to the protocols approved by the Institutional Animal Care and Use Committees at the University of Texas Southwestern Medical Center.

NIH3T3, HEK293/T17, mouse embryonic fibroblasts (MEFs), *PER2::LUC* MEFs, and *Bmal1-luc* cells were grown in Dulbecco's modified Eagle medium (Life Technologies) with 10% fetal bovine serum (FBS) (Atlanta Biologicals) at 37°C with 5% CO_2. AML12 cells were grown in Dulbecco's modified Eagle medium/F12 (1:1) with 10% FBS and 1% insulin–transferrin–selenium supplement (Gibco) at 37°C with 5% CO_2.

Chromosomal numbers were counted as previous reported (Nicholson et al. 2015) with minor modifications. Briefly, cell cultures were incubated in 1000 ng/mL Colcemid (Karyomax, Invitrogen) for 3–6 h at 37°C to enrich in mitotically arrested cells. The cells were then collected by centrifugation, and prewarmed hypotonic solution (0.075M KCl) was added drop-wise to the cell pellet. After incubation for 18 min at 37°C, cells were fixed with an ice-cold 3:1 methanol:acetic acid solution for 5 min followed by centrifugation. After repeating this last step twice, fixed cells were dropped on microscope slides.

CRISPR mutagenesis

The sgRNAs were designed by the CRISPR design tool (http://crispr.mit.edu), and complementary oligonucleotides were annealed, phosphorylated, and cloned into the BbsI sites of the pSpCas9(BB)-2A-GFP (Addgene plasmid 48138) (Ran et al. 2013). After the nucleotide sequences of the plasmids were verified by Sanger sequencing, DNA was transfected into *PER2::LUC* MEFs and/or *Bmal1-luc* cells using FuGENE6 according to the manufacturer's instructions. After 48 h, cells were trypsinized and sorted using FACSAria I (BD Biosciences) with GFP signals. Subsequently, cells were cultured in DMEM supplemented with 10% FBS and 1× penicillin/streptomycin (Gibco). When each clone reached confluency, cells were lysed with 90 µL of 50 mM NaOH and 10 µL of 100 mM Tris-HCl (pH 8.0), followed by incubation for 10 min at 95°C. The mutated genomic region was first amplified by PCR, then cloned into the pGEM-T vector (Promega), to reveal the nucleotide sequence of each clone by Sanger sequence. All the primer sequences used in this study are in Supplemental Table S1.

Real-time bioluminescence recordings and luciferase assay

Cells were first plated into 35-mm dishes and then allowed to become confluent. The medium was then replaced with DMEM

supplemented with 50% horse serum (gene expression analyses) or dexamethasone (1 μM) was added to the media (real-time bioluminescence recordings) for 2 h. After synchronizing cells, medium was changed to phenol red-free DMEM (Cellgro 90-013-PB) supplemented with 100 μM luciferrin, 10 mM HEPES (pH 7.2), 1 mM sodium pyruvate, 0.035% sodium bicarbonate, 2% FBS, 1× penicillin/streptomycin, and 2 mM L-glutamine. Real-time bioluminescence recordings were performed using a LumiCycle (Actimetrics, Inc.). Quantification analyses was performed by JMP software (Oklejewicz et al. 2008). The recordings from the first 24 h were eliminated for quantitative analyses because these data are unreliable.

Luciferase assays were performed as previously reported (Kojima et al. 2010). Briefly, a mixture of plasmid DNAs containing 100 ng of *Per2E2-luc* or *Bmal1-luc* firefly luciferase reporter genes, 10 ng of *Renilla* luciferase reporter genes, and increasing amounts of *Per2AS* (variant2)-expressing plasmids (50, 100, 200, and 400 ng) were cotransfected in NIH3T3 cells. Luciferase activities were measured ~48 h after transfection. The *Per2E2-luc* reporter gene was constructed by inserting the mouse *Per2* promoter (−83 to +156 in reference to the *Per2* TSS) into pGL4.12[*luc2CP*] (Promega), whereas *Bmal1-luc* was constructed by inserting the mouse *Bmal1* promoter (−779 to +127 in reference to the *Bmal1* TSS) into pGL4.11[*luc2P*] (Promega).

RT-qPCRTotal RNA was extracted with TRIZOL reagent (Life Technologies) according to the manufacturer's instructions and treated with TURBO DNaseI (Life Technologies). RNAs were then subjected to reverse transcription using SuperScript II (Life Technologies) or high-capacity cDNA reverse transcription kits (Applied Biosystems). For *Per2AS* transcripts, cDNA was synthesized using strand-specific primers (Supplemental Table S1), except for Figure 1A, in which the oligo(dT) was used. qPCR was performed using QuantiStudio 6 (Life Technologies) with SYBR Power Green (Applied Biosystems). All the primer sequences used in this study are in Supplemental Table S1.

Rapid amplification of cDNA ends assay

A RACE assay was performed with a SMARTer RACE 5′/3′ kit (Clontech) according to the manufacturer's instructions. Total RNAs from mouse liver (C57BL/6J) harvested at ZT4 was subjected to 5′- and 3′-RACE cDNA synthesis. Each cDNA was then amplified by *Per2AS*-specific primers (Supplemental Table S1) together with the Universal Primer (Clontech). The first PCR products were subsequently amplified by the nested *Per2AS*-specific primers with Universal Primer (Clontech). The nested PCR products were cloned into the pGEM-T vector (Promega), and the nucleotide sequence was determined by Sanger sequencing. Two independent 5′RACE products had the identical sequence, while four 3′RACE products yielded three different sequences, giving rise to the three variants of *Per2AS* (Fig. 1B; Supplemental Fig. S1C).

Northern blotting

Total RNA (~500 μg) extracted from mouse liver harvested at ZT4, at which *Per2AS* expression is the highest (Koike et al. 2012), was subjected to a poly(A)$^+$tract isolation kit (Promega). Poly(A)$^+$ enriched RNA, as well as the RNA ladder (Life Technologies), were further separated on a 1% agarose gel, transferred to Hybond-N$^+$ membrane (Amersham), and UV cross-linked (Stratagene) using a standard protocol. The membrane was further hybridized overnight at 68°C using PerfectHyb PLUS (Sigma) with a P^{32}UTP-labeled probe that has a complementary sequence against *Per2AS* (1–1812 nt) (Fig. 1B; Supplemental Fig. S1C), where all the variants share its nucleotide sequences. After extensive washing of the membrane, the radioactive signal was analyzed with a Storm image analyzer (GE Healthcare).

Subcellular fractionation

Livers from mice (C57BL/6J) were immediately rinsed with an ice-cold 0.9% NaCl solution, then homogenized on ice with five volumes of homogenization buffer (10 mM Tris-HCl buffer at pH 7.7, containing 10 mM NaCl, 0.1 mM EGTA, 0.5 mM EDTA, 0.5 mM spermidine, 0.15 mM spermine, 0.5% Tergitol NP-10, 1 mM dithiothreitol, 1 mM phenylmethylsulfonyl fluoride) in a Dounce homogenizer. The homogenates were filtered through two layers of cheesecloth and, following dilution with eight tissue volumes of 2.2 M sucrose in the homogenization buffer, applied to a 10-mL cushion of 2 M sucrose in homogenization buffer and spun at 24,000 rpm for 60 min at 2°C in a prechilled SW28 rotor. The resultant nuclear pellet as well as the supernatant were subjected to RNA extraction. For NIH3T3 and MEFs, cells were lysed in an ice-cold hypotonic lysis buffer (10 mM Tris-HCl at pH 7.4, 10 mM NaCl, 3 mM $MgCl_2$, 0.3% NP-40) supplemented with protease inhibitor cocktail (Sigma). After incubation for 5 min on ice with occasional pipetting, lysates were separated into nuclear and cytoplasmic fractions by centrifuging at 600*g* for 5 min at 4°C. RNAs were extracted from each fraction using Trizol reagent (Life Technologies) and subjected to RT-qPCR.

Per2AS overexpression and knockdown

A *Per2AS* variant 2 overexpression plasmid was generated from 5′RACE and 3′RACE products that were cloned into pBluescript (Agilent), as well as *Per2AS* qPCR product cloned into pGEM-T (Promega). After combining 5′RACE and qPCR products in pBlueScript using HindIII and XhoI sites, the 3′RACE product was also inserted using XhoI and KpnI sites. The full length was then transferred to pcDNA3.1-mycHis (Invitrogen), and its sequence was verified by Sanger sequencing. DNA transfection was performed with either FuGENE6 Reagent (Promega) or Lipofectamine 2000 (Life Technologies) using Opti-MEM (Gibco), while gapmers were introduced via gymnosis (Stein et al. 2010) with the final concentration of 100 nM (Supplemental Table S1).

Lentivirus generation and transduction

For virus production, either control or *Per2* shRNA as well as viral packaging vectors were transfected into HEK293/T17 cells according to the manufacturer's instruction (ViraPower Lentiviral Expression System, Life Technologies). Cell culture media was collected after 48 h, ultracentrifuged at 70,000*g* for 2 h at room temperature, then resuspended in target cell-specific media. Viral media and 20 μg/mL polybrene (Millipore) were added to target cells, and cells were harvested 48–72 h after viral transduction.

Mathematical model

Our model of *Per2-Per2AS* interactions (Battogtokh et al. 2018) was based on an earlier model (Relogio et al. 2011) of the mammalian circadian clock, which did not take *Per2AS* into account. Our model of the basic negative feedback loop, whereby PER2:CRY inhibits BMAL:CLOCK (without additional feedback loops through REV-ERB and ROR), consisted of 15 ordinary differential equations (ODEs) with 44 parameter values (rate constants, binding constants, etc.). To illustrate some of the results of this detailed model, we present here a simpler model of the negative

feedback loop (Supplemental Fig. S6A) based on Goodwin's original model (Goodwin 1965), with an important modification suggested by Bliss, Painter, and Marr (Bliss et al. 1982). *Per2AS* RNA was added to the basic Goodwin model by assuming that *Per2AS* and *Per2* mutually inhibit each other pretranscriptionally. The ODEs describing the model are presented in Supplemental Figure S6B. The model with *Per2AS* consists of all four ODEs, as written. The model without *Per2AS* consists of the first three ODEs only, and the blue factor in the first ODE is set = 1. These two models were simulated with the XPP-AUT program (http://www.math.pitt.edu/~bard/xpp/xpp.html) using the parameter values given in Supplemental Table S2. The parameter values were chosen to give oscillations with a period close to 24 h and reasonable amplitudes and phase relations of the variables (Supplemental Fig. S6C. In particular, the model with *Per2AS* was constrained to fit experimental observations in mouse liver that the level of *Per2AS* is ~5% of *Per2* and that *Per2AS* and *Per2* are expressed antiphasically (Koike et al. 2012). In Supplemental Figure S6D we compare the robustness of oscillations in the models with and without *Per2AS*, in terms of the range of a_1 values (the maximum rate of synthesis of *Per2* mRNA) over which the models exhibit oscillations. By this measure, the model with *Per2AS* is considerably more robust than the model without *Per2AS*. In Supplemental Figure S6E, we show the domains of oscillation for both models on a two-parameter diagram: a_1 and b_3, where b_3 is the maximum rate of degradation of phosphorylated PER2 in the nucleus. This diagram also shows a larger region of oscillations in the model with *Per2AS*. Even if we restrict our attention to the regions of "circadian" oscillations (22 < period [h] < 26) in parameter space, the model with *Per2AS* (blue lines in Supplemental Fig. S6E) is noticeably more robust than the model without *Per2AS* (black lines).

Competing interest statement

The authors declare no competing interests.

Acknowledgment

We thank Dr. Ueli Schibler (Université de Genève) for providing the *Bmal1-luc* cell line, Dr. Seung-Hee Yoo (University of Texas Health Science Center at Houston) for *PER2::LUC* MEFs, and Dr. Andrew Liu (University of Florida) for *Per2* shRNA vectors (Ramanathan et al. 2014). We also thank Melissa Makris (Flow Cytometry Resource Laboratory, Department of Biomedical Sciences and Pathobiology, Center for Molecular Medicine and Infectious Diseases, Virginia-Maryland Regional College of Veterinary Medicine, Virginia Polytechnic Institute and State University), Dr. Nicolaas Baudoin and Dr. Daniela Cimini (Department of Biological Sciences, Virginia Polytechnic Institute and State University), and Tsubasa Toda and Akari Ueta (Department of Environmental and Life Sciences, Toyohashi University of Technology) for technical assistance. We also thank all the past an current members of the Green, Takahashi, and Kojima laboratories for invaluable discussion. This work was supported by the Luther and Alice Hamlett Undergraduate Research Support (to C.T.S), Howard Hughes Medical Institute (to J.S.T), and National Institutes of Health GM127122 (to C.B.G), and GM126223 (to S.K.). J.S.T. is an Investigator in the Howard Hughes Medical Institute.

Author contributions: R.A.M., A.N.C., J.C.D., L.P.F., K.L.H., N.M., A.P., C.T.S., L.Z., N.K., J.J.T., and S.K. acquired, analyzed, and interpreted the data. R.A.M., N.K., J.J.T., C.B.G., J.S.T., and S.K., drafted the work and/or critically revised the manuscript for intellectual content. All the authors approved of the manuscript and are accountable for the scientific integrity.

References

Anderson KM, Anderson DM, McAnally JR, Shelton JM, Bassel-Duby R, Olson EN. 2016. Transcription of the non-coding RNA upperhand controls Hand2 expression and heart development. *Nature* **539:** 433–436. doi:10.1038/nature20128

Atger F, Gobet C, Marquis J, Martin E, Wang J, Weger B, Lefebvre G, Descombes P, Naef F, Gachon F. 2015. Circadian and feeding rhythms differentially affect rhythmic mRNA transcription and translation in mouse liver. *Proc Natl Acad Sci* **112:** E6579–E6588. doi:10.1073/pnas.1515308112

Bae K, Jin X, Maywood ES, Hastings MH, Reppert SM, Weaver DR. 2001. Differential functions of mPer1, mPer2, and mPer3 in the SCN circadian clock. *Neuron* **30:** 525–536. doi:10.1016/S0896-6273(01)00302-6

Baggs JE, Price TS, DiTacchio L, Panda S, Fitzgerald GA, Hogenesch JB. 2009. Network features of the mammalian circadian clock. *PLoS Biol* **7:** e1000052. doi:10.1371/journal.pbio.1000052

Balsalobre A, Damiola F, Schibler U. 1998. A serum shock induces circadian gene expression in mammalian tissue culture cells. *Cell* **93:** 929–937. doi:10.1016/S0092-8674(00)81199-X

Battogtokh D, Kojima S, Tyson JJ. 2018. Modeling the interactions of sense and antisense period transcripts in the mammalian circadian clock network. *PLoS Comput Biol* **14:** e1005957. doi:10.1371/journal.pcbi.1005957

Bertone P, Stolc V, Royce TE, Rozowsky JS, Urban AE, Zhu X, Rinn JL, Tongprasit W, Samanta M, Weissman S, et al. 2004. Global identification of human transcribed sequences with genome tiling arrays. *Science* **306:** 2242–2246. doi:10.1126/science.1103388

Bliss RD, Painter PR, Marr AG. 1982. Role of feedback inhibition in stabilizing the classical operon. *J Theor Biol* **97:** 177–193. doi:10.1016/0022-5193(82)90098-4

Bond AM, Vangompel MJ, Sametsky EA, Clark MF, Savage JC, Disterhoft JF, Kohtz JD. 2009. Balanced gene regulation by an embryonic brain ncRNA is critical for adult hippocampal GABA circuitry. *Nat Neurosci* **12:** 1020–1027. doi:10.1038/nn.2371

Carninci P, Kasukawa T, Katayama S, Gough J, Frith MC, Maeda N, Oyama R, Ravasi T, Lenhard B, Wells C, et al. 2005. The transcriptional landscape of the mammalian genome. *Science* **309:** 1559–1563. doi:10.1126/science.1112014

Carthew RW, Sontheimer EJ. 2009. Origins and mechanisms of miRNAs and siRNAs. *Cell* **136:** 642–655. doi:10.1016/j.cell.2009.01.035

Chen LL. 2016. Linking long noncoding RNA localization and function. *Trends Biochem Sci* **41:** 761–772. doi:10.1016/j.tibs.2016.07.003

Chen R, Schirmer A, Lee Y, Lee H, Kumar V, Yoo SH, Takahashi JS, Lee C. 2009. Rhythmic PER abundance defines a critical nodal point for negative feedback within the circadian clock mechanism. *Mol Cell* **36:** 417–430. doi:10.1016/j.molcel.2009.10.012

Clemson CM, Hutchinson JN, Sara SA, Ensminger AW, Fox AH, Chess A, Lawrence JB. 2009. An architectural role for a nuclear noncoding RNA: NEAT1 RNA is essential for the structure of paraspeckles. *Mol Cell* **33:** 717–726. doi:10.1016/j.molcel.2009.01.026

Davis CA, Hitz BC, Sloan CA, Chan ET, Davidson JM, Gabdank I, Hilton JA, Jain K, Baymuradov UK, Narayanan AK, et al. 2018.

The Encyclopedia of DNA Elements (ENCODE): data portal update. *Nucleic Acids Res* **46:** D794–D801. doi:10.1093/nar/gkx1081

Derrien T, Johnson R, Bussotti G, Tanzer A, Djebali S, Tilgner H, Guernec G, Martin D, Merkel A, Knowles DG, et al. 2012. The GENCODE v7 catalog of human long noncoding RNAs: analysis of their gene structure, evolution, and expression. *Genome Res* **22:** 1775–1789. doi:10.1101/gr.132159.111

Dinger ME, Amaral PP, Mercer TR, Pang KC, Bruce SJ, Gardiner BB, Askarian-Amiri ME, Ru K, Solda G, Simons C, et al. 2008. Long noncoding RNAs in mouse embryonic stem cell pluripotency and differentiation. *Genome Res* **18:** 1433–1445. doi:10.1101/gr.078378.108

Djebali S, Davis CA, Merkel A, Dobin A, Lassmann T, Mortazavi A, Tanzer A, Lagarde J, Lin W, Schlesinger F, et al. 2012. Landscape of transcription in human cells. *Nature* **489:** 101–108. doi:10.1038/nature11233

The ENCODE Project Consortium. 2012. An integrated encyclopedia of DNA elements in the human genome. *Nature* **489:** 57–74. doi:10.1038/nature11247

Engreitz JM, Haines JE, Perez EM, Munson G, Chen J, Kane M, McDonel PE, Guttman M, Lander ES. 2016. Local regulation of gene expression by lncRNA promoters, transcription and splicing. *Nature* **539:** 452–455. doi:10.1038/nature20149

Faghihi MA, Wahlestedt C. 2009. Regulatory roles of natural antisense transcripts. *Nat Rev Mol Cell Biol* **10:** 637–643. doi:10.1038/nrm2738

Fang B, Everett LJ, Jager J, Briggs E, Armour SM, Feng D, Roy A, Gerhart-Hines Z, Sun Z, Lazar MA. 2014. Circadian enhancers coordinate multiple phases of rhythmic gene transcription in vivo. *Cell* **159:** 1140–1152. doi:10.1016/j.cell.2014.10.022

Feng J, Bi C, Clark BS, Mady R, Shah P, Kohtz JD. 2006. The Evf-2 noncoding RNA is transcribed from the Dlx-5/6 ultraconserved region and functions as a Dlx-2 transcriptional coactivator. *Genes Dev* **20:** 1470–1484. doi:10.1101/gad.1416106

Goodman AJ, Daugharthy ER, Kim J. 2013. Pervasive antisense transcription is evolutionarily conserved in budding yeast. *Mol Biol Evol* **30:** 409–421. doi:10.1093/molbev/mss240

Goodwin BC. 1965. Oscillatory behavior in enzymatic control processes. *Adv Enzyme Regul* **3:** 425–437. doi:10.1016/0065-2571(65)90067-1

Groff AF, Sanchez-Gomez DB, Soruco MML, Gerhardinger C, Barutcu AR, Li E, Elcavage L, Plana O, Sanchez LV, Lee JC, et al. 2016. In vivo characterization of Linc-p21 reveals functional *cis*-regulatory DNA elements. *Cell Rep* **16:** 2178–2186. doi:10.1016/j.celrep.2016.07.050

Guttman M, Amit I, Garber M, French C, Lin MF, Feldser D, Huarte M, Zuk O, Carey BW, Cassady JP, et al. 2009. Chromatin signature reveals over a thousand highly conserved large non-coding RNAs in mammals. *Nature* **458:** 223–227. doi:10.1038/nature07672

Halley P, Kadakkuzha BM, Faghihi MA, Magistri M, Zeier Z, Khorkova O, Coito C, Hsiao J, Lawrence M, Wahlestedt C. 2014. Regulation of the apolipoprotein gene cluster by a long noncoding RNA. *Cell Rep* **6:** 222–230. doi:10.1016/j.celrep.2013.12.015

He Y, Vogelstein B, Velculescu VE, Papadopoulos N, Kinzler KW. 2008. The antisense transcriptomes of human cells. *Science* **322:** 1855–1857. doi:10.1126/science.1163853

He B, Nohara K, Park N, Park YS, Guillory B, Zhao Z, Garcia JM, Koike N, Lee CC, Takahashi JS, et al. 2016. The small molecule Nobiletin targets the molecular oscillator to enhance circadian rhythms and protect against metabolic syndrome. *Cell Metab* **23:** 610–621. doi:10.1016/j.cmet.2016.03.007

Janich P, Arpat AB, Castelo-Szekely V, Lopes M, Gatfield D. 2015. Ribosome profiling reveals the rhythmic liver translatome and circadian clock regulation by upstream open reading frames. *Genome Res* **25:** 1848–1859. doi:10.1101/gr.195404.115

Johnsson P, Lipovich L, Grandér D, Morris KV. 2014. Evolutionary conservation of long non-coding RNAs; sequence, structure, function. *Biochim Biophys Acta* **1840:** 1063–1071. doi:10.1016/j.bbagen.2013.10.035

Kaikkonen MU, Adelman K. 2018. Emerging roles of non-coding RNA transcription. *Trends Biochem Sci* **43:** 654–667. doi:10.1016/j.tibs.2018.06.002

Katayama S, Tomaru Y, Kasukawa T, Waki K, Nakanishi M, Nakamura M, Nishida H, Yap CC, Suzuki M, Kawai J, et al. 2005. Antisense transcription in the mammalian transcriptome. *Science* **309:** 1564–1566. doi:10.1126/science.1112009

Khaitovich P, Kelso J, Franz H, Visagie J, Giger T, Joerchel S, Petzold E, Green RE, Lachmann M, Pääbo S. 2006. Functionality of intergenic transcription: an evolutionary comparison. *PLoS Genet* **2:** e171. doi:10.1371/journal.pgen.0020171

Khorkova O, Myers AJ, Hsiao J, Wahlestedt C. 2014. Natural antisense transcripts. *Hum Mol Genet* **23:** R54–R63. doi:10.1093/hmg/ddu207

Koike N, Yoo SH, Huang HC, Kumar V, Lee C, Kim TK, Takahashi JS. 2012. Transcriptional architecture and chromatin landscape of the core circadian clock in mammals. *Science* **338:** 349–354. doi:10.1126/science.1226339

Kojima S, Gatfield D, Esau CC, Green CB. 2010. MicroRNA-122 modulates the rhythmic expression profile of the circadian deadenylase Nocturnin in mouse liver. *PLoS One* **5:** e11264. doi:10.1371/journal.pone.0011264

Kramer C, Loros JJ, Dunlap JC, Crosthwaite SK. 2003. Role for antisense RNA in regulating circadian clock function in *Neurospora crassa*. *Nature* **421:** 948–952. doi:10.1038/nature01427

Lee JS, Mendell JT. 2020. Antisense-mediated transcript knockdown triggers premature transcription termination. *Mol Cell* **77:** 1044–1054.e3. doi:10.1016/j.molcel.2019.12.011

Lee JT, Davidow LS, Warshawsky D. 1999. *Tsix*, a gene antisense to *Xist* at the X-inactivation centre. *Nat Genet* **21:** 400–404. doi:10.1038/7734

Lee JE, Bennett CF, Cooper TA. 2012. RNase H-mediated degradation of toxic RNA in myotonic dystrophy type 1. *Proc Natl Acad Sci* **109:** 4221–4226. doi:10.1073/pnas.1117019109

Littleton ES, Childress ML, Gosting ML, Jackson AN, Kojima S. 2020. Genome-wide correlation analysis to identify amplitude regulators of circadian transcriptome output. *Sci Rep* **10:** 21839. doi:10.1038/s41598-020-78851-9

Liu AC, Welsh DK, Ko CH, Tran HG, Zhang EE, Priest AA, Buhr ED, Singer O, Meeker K, Verma IM, et al. 2007. Intercellular coupling confers robustness against mutations in the SCN circadian clock network. *Cell* **129:** 605–616. doi:10.1016/j.cell.2007.02.047

Lowrey PL, Takahashi JS. 2004. Mammalian circadian biology: elucidating genome-wide levels of temporal organization. *Annu Rev Genomics Hum Genet* **5:** 407–441. doi:10.1146/annurev.genom.5.061903.175925

Luck S, Thurley K, Thaben PF, Westermark PO. 2014. Rhythmic degradation explains and unifies circadian transcriptome and proteome data. *Cell Rep* **9:** 741–751. doi:10.1016/j.celrep.2014.09.021

Marchese FP, Raimondi I, Huarte M. 2017. The multidimensional mechanisms of long noncoding RNA function. *Genome Biol* **18:** 206. doi:10.1186/s13059-017-1348-2

Menet JS, Rodriguez J, Abruzzi KC, Rosbash M. 2012. Nascent-Seq reveals novel features of mouse circadian transcriptional regulation. *Elife* **1:** e00011. doi:10.7554/eLife.00011

Mercer TR, Dinger ME, Mattick JS. 2009. Long non-coding RNAs: insights into functions. *Nat Rev Genet* **10:** 155–159. doi:10.1038/nrg2521

Modarresi F, Faghihi MA, Lopez-Toledano MA, Fatemi RP, Magistri M, Brothers SP, van der Brug MP, Wahlestedt C. 2012. Inhibition of natural antisense transcripts in vivo results in gene-specific transcriptional upregulation. *Nat Biotechnol* **30:** 453–459. doi:10.1038/nbt.2158

Morf J, Rey G, Schneider K, Stratmann M, Fujita J, Naef F, Schibler U. 2012. Cold-inducible RNA-binding protein modulates circadian gene expression posttranscriptionally. *Science* **338:** 379–383. doi:10.1126/science.1217726

Morris KV, Santoso S, Turner AM, Pastori C, Hawkins PG. 2008. Bidirectional transcription directs both transcriptional gene activation and suppression in human cells. *PLoS Genet* **4:** e1000258. doi:10.1371/journal.pgen.1000258

Nicholson JM, Macedo JC, Mattingly AJ, Wangsa D, Camps J, Lima V, Gomes AM, Dória S, Ried T, Logarinho E, et al. 2015. Chromosome mis-segregation and cytokinesis failure in trisomic human cells. *Elife* **4:** e05068. doi:10.7554/eLife.05068

Oklejewicz M, Destici E, Tamanini F, Hut RA, Janssens R, van der Horst GT. 2008. Phase resetting of the mammalian circadian clock by DNA damage. *Curr Biol* **18:** 286–291. doi:10.1016/j.cub.2008.01.047

Panda AC, Grammatikakis I, Munk R, Gorospe M, Abdelmohsen K. 2017. Emerging roles and context of circular RNAs. *Wiley Interdiscip Rev RNA* **8:** e1386. doi:10.1002/wrna.1386

Pang KC, Frith MC, Mattick JS. 2006. Rapid evolution of noncoding RNAs: lack of conservation does not mean lack of function. *Trends Genet* **22:** 1–5. doi:10.1016/j.tig.2005.10.003

Pendergast JS, Friday RC, Yamazaki S. 2010. Distinct functions of Period2 and Period3 in the mouse circadian system revealed by in vitro analysis. *PLoS One* **5:** e8552. doi:10.1371/journal.pone.0008552

Phatnani HP, Greenleaf AL. 2006. Phosphorylation and functions of the RNA polymerase II CTD. *Genes Dev* **20:** 2922–2936. doi:10.1101/gad.1477006

Ponjavic J, Ponting CP, Lunter G. 2007. Functionality or transcriptional noise? Evidence for selection within long noncoding RNAs. *Genome Res* **17:** 556–565. doi:10.1101/gr.6036807

Ramanathan C, Xu H, Khan SK, Shen Y, Gitis PJ, Welsh DK, Hogenesch JB, Liu AC. 2014. Cell type-specific functions of period genes revealed by novel adipocyte and hepatocyte circadian clock models. *PLoS Genet* **10:** e1004244. doi:10.1371/journal.pgen.1004244

Ran FA, Hsu PD, Wright J, Agarwala V, Scott DA, Zhang F. 2013. Genome engineering using the CRISPR-Cas9 system. *Nat Protoc* **8:** 2281–2308. doi:10.1038/nprot.2013.143

Relogio A, Westermark PO, Wallach T, Schellenberg K, Kramer A, Herzel H. 2011. Tuning the mammalian circadian clock: robust synergy of two loops. *PLoS Comput Biol* **7:** e1002309. doi:10.1371/journal.pcbi.1002309

Rhind N, Chen Z, Yassour M, Thompson DA, Haas BJ, Habib N, Wapinski I, Roy S, Lin MF, Heiman DI, et al. 2011. Comparative functional genomics of the fission yeasts. *Science* **332:** 930–936. doi:10.1126/science.1203357

Røsok O, Sioud M. 2004. Systematic identification of sense-antisense transcripts in mammalian cells. *Nat Biotechnol* **22:** 104–108. doi:10.1038/nbt925

Sato TK, Panda S, Miraglia LJ, Reyes TM, Rudic RD, McNamara P, Naik KA, FitzGerald GA, Kay SA, Hogenesch JB. 2004. A functional genomics strategy reveals Rora as a component of the mammalian circadian clock. *Neuron* **43:** 527–537. doi:10.1016/j.neuron.2004.07.018

Sauman I, Reppert SM. 1996. Circadian clock neurons in the silkmoth *Antheraea pernyi*: novel mechanisms of Period protein regulation. *Neuron* **17:** 889–900. doi:10.1016/S0896-6273(00)80220-2

Schmutz I, Ripperger JA, Baeriswyl-Aebischer S, Albrecht U. 2010. The mammalian clock component PERIOD2 coordinates circadian output by interaction with nuclear receptors. *Genes Dev* **24:** 345–357. doi:10.1101/gad.564110

Shearman LP, Sriram S, Weaver DR, Maywood ES, Chaves I, Zheng B, Kume K, Lee CC, van der Horst GT, Hastings MH, et al. 2000. Interacting molecular loops in the mammalian circadian clock. *Science* **288:** 1013–1019. doi:10.1126/science.288.5468.1013

Sleutels F, Zwart R, Barlow DP. 2002. The non-coding Air RNA is required for silencing autosomal imprinted genes. *Nature* **415:** 810–813. doi:10.1038/415810a

Smilinich NJ, Day CD, Fitzpatrick GV, Caldwell GM, Lossie AC, Cooper PR, Smallwood AC, Joyce JA, Schofield PN, Reik W, et al. 1999. A maternally methylated CpG island in KvLQT1 is associated with an antisense paternal transcript and loss of imprinting in Beckwith-Wiedemann syndrome. *Proc Natl Acad Sci* **96:** 8064–8069. doi:10.1073/pnas.96.14.8064

Sopher BL, Ladd PD, Pineda VV, Libby RT, Sunkin SM, Hurley JB, Thienes CP, Gaasterland T, Filippova GN, La Spada AR. 2011. CTCF regulates ataxin-7 expression through promotion of a convergently transcribed, antisense noncoding RNA. *Neuron* **70:** 1071–1084. doi:10.1016/j.neuron.2011.05.027

Stein CA, Hansen JB, Lai J, Wu S, Voskresenskiy A, Hø g A, Worm J, Hedtjärn M, Souleimanian N, Miller P, et al. 2010. Efficient gene silencing by delivery of locked nucleic acid antisense oligonucleotides, unassisted by transfection reagents. *Nucleic Acids Res* **38:** e3. doi:10.1093/nar/gkp841

Sun M, Hurst LD, Carmichael GG, Chen J. 2006. Evidence for variation in abundance of antisense transcripts between multicellular animals but no relationship between antisense transcriptionand organismic complexity. *Genome Res* **16:** 922–933. doi:10.1101/gr.5210006

Takahashi JS. 2017. Transcriptional architecture of the mammalian circadian clock. *Nat Rev Genet* **18:** 164–179. doi:10.1038/nrg.2016.150

Takahashi JS, Hong HK, Ko CH, McDearmon EL. 2008. The genetics of mammalian circadian order and disorder: implications for physiology and disease. *Nat Rev Genet* **9:** 764–775. doi:10.1038/nrg2430

Tamiya H, Ogawa S, Ouchi Y, Akishita M. 2016. Rigid cooperation of Per1 and Per2 proteins. *Sci Rep* **6:** 32769. doi:10.1038/srep32769

Villegas VE, Rahman MF, Fernandez-Barrena MG, Diao Y, Liapi E, Sonkoly E, Ståhle M, Pivarcsi A, Annaratone L, Sapino A, et al. 2014. Identification of novel non-coding RNA-based negative feedback regulating the expression of the oncogenic transcription factor GLI1. *Mol Oncol* **8:** 912–926. doi:10.1016/j.molonc.2014.03.009

Vitaterna MH, Ko CH, Chang AM, Buhr ED, Fruechte EM, Schook A, Antoch MP, Turek FW, Takahashi JS. 2006. The mouse Clock mutation reduces circadian pacemaker amplitude and enhances efficacy of resetting stimuli and phase-response curve amplitude. *Proc Natl Acad Sci* **103:** 9327–9332. doi:10.1073/pnas.0603601103

Vollmers C, Schmitz RJ, Nathanson J, Yeo G, Ecker JR, Panda S. 2012. Circadian oscillations of protein-coding and regulatory

RNAs in a highly dynamic mammalian liver epigenome. *Cell Metab* **16:** 833–845. doi:10.1016/j.cmet.2012.11.004

Wanowska E, Kubiak MR, Rosikiewicz W, Makałowska I, Szcześniak MW. 2018. Natural antisense transcripts in diseases: from modes of action to targeted therapies. *Wiley Interdiscip Rev RNA* **9:** e1461. doi:10.1002/wrna.1461

Wight M, Werner A. 2013. The functions of natural antisense transcripts. *Essays Biochem* **54:** 91–101. doi:10.1042/bse0540091

Xu Z, Wei W, Gagneur J, Perocchi F, Clauder-Münster S, Camblong J, Guffanti E, Stutz F, Huber W, Steinmetz LM. 2009. Bidirectional promoters generate pervasive transcription in yeast. *Nature* **457:** 1033–1037. doi:10.1038/nature07728

Xu Z, Wei W, Gagneur J, Clauder-Münster S, Smolik M, Huber W, Steinmetz LM. 2011. Antisense expression increases gene expression variability and locus interdependency. *Mol Syst Biol* **7:** 468. doi:10.1038/msb.2011.1

Xue Z, Ye Q, Anson SR, Yang J, Xiao G, Kowbel D, Glass NL, Crosthwaite SK, Liu Y. 2014. Transcriptional interference by antisense RNA is required for circadian clock function. *Nature* **514:** 650–653. doi:10.1038/nature13671

Yassour M, Pfiffner J, Levin JZ, Adiconis X, Gnirke A, Nusbaum C, Thompson DA, Friedman N, Regev A. 2010. Strand-specific RNA sequencing reveals extensive regulated long antisense transcripts that are conserved across yeast species. *Genome Biol* **11:** R87. doi:10.1186/gb-2010-11-8-r87

Yoo SH, Yamazaki S, Lowrey PL, Shimomura K, Ko CH, Buhr ED, Siepka SM, Hong HK, Oh WJ, Yoo OJ, et al. 2004. PERIOD2::LUCIFERASE real-time reporting of circadian dynamics reveals persistent circadian oscillations in mouse peripheral tissues. *Proc Natl Acad Sci* **101:** 5339–5346. doi:10.1073/pnas.0308709101

Yoo SH, Kojima S, Shimomura K, Koike N, Buhr ED, Furukawa T, Ko CH, Gloston G, Ayoub C, Nohara K, et al. 2017. *Period2* 3′-UTR and microRNA-24 regulate circadian rhythms by repressing PERIOD2 protein accumulation. *Proc Natl Acad Sci* **114:** E8855–E8864. doi:10.1073/pnas.1706611114

Zhang EE, Liu AC, Hirota T, Miraglia LJ, Welch G, Pongsawakul PY, Liu X, Atwood A, Huss JW, Janes J, et al. 2009. A genome-wide RNAi screen for modifiers of the circadian clock in human cells. *Cell* **139:** 199–210. doi:10.1016/j.cell.2009.08.031

Zhang R, Lahens NF, Ballance HI, Hughes ME, Hogenesch JB. 2014. A circadian gene expression atlas in mammals: implications for biology and medicine. *Proc Natl Acad Sci* **111:** 16219–16224. doi:10.1073/pnas.1408886111

Zhao J, Sun BK, Erwin JA, Song JJ, Lee JT. 2008. Polycomb proteins targeted by a short repeat RNA to the mouse X chromosome. *Science* **322:** 750–756. doi:10.1126/science.1163045

Zhao X, Hirota T, Han X, Cho H, Chong LW, Lamia K, Liu S, Atkins AR, Banayo E, Liddle C, et al. 2016. Circadian amplitude regulation via FBXW7-targeted REV-ERBα degradation. *Cell* **165:** 1644–1657. doi:10.1016/j.cell.2016.05.012

Zheng B, Larkin DW, Albrecht U, Sun ZS, Sage M, Eichele G, Lee CC, Bradley A. 1999. The mPer2 gene encodes a functional component of the mammalian circadian clock. *Nature* **400:** 169–173. doi:10.1038/22118